

AD

**STUDY OF THE BOUNDARY LAYER IN THE INBOARD SECTIONS OF A  
TILT-ROTOR BLADE BY EMBEDDED LDV MEASUREMENTS**

Final Technical Report

by

Christian. Maresca, Marcellin. Nsi Mbà, Eric. Berton, Daniel. Favier, and  
Charlie Barla

Laboratoire d'Aérodynamique et de Biomécanique du Mouvement  
163 Av. de Luminy, Case 918  
13288 marseille cedex 09. France

(July 2003)

United States Army

EUROPEAN RESEARCH OFFICE OF THE U.S. ARMY

London, England

CONTRACT NUMBER N 62558-02-M-5609

Contractor: M. Laurent, Président de l'Université de la Méditerranée

Approved for Public Release; distribution unlimited

20040219 177

## REPORT DOCUMENTATION PAGE

9327AN01

1. Agency Use Only	2. Report Date : 25 JULY 2003	3. Type of Report and Dates Covered : Final Report 6 May 2002-JUL2003	
4. Titles and Subtitle: Study of the boundary layer in the inboard region of a tilt-rotor blade by embedded LDV measurements.		5. Funding Numbers : C N 62558-02-M5609	
6. Author(s): C. Maresca, M. Nsi Mba , E. Berton, D. Favier, and C. Barla			
7. Performing Organization Name(s) and Adresse(s) : LABM, CNRS-University of la Méditerranée. 163 Av. de Luminy, Case 918 13288 Marseille, Cedex 009, France		8. Performing Organization Report Number : 03-00-16-8	
9. Sponsoring/Monitoring Agency Name(s) and Adresse(s)		10. Sponsoring/Monitoring Agency Report	
11. Supplementary notes			
12a. Distribution/Availability Statement public availability		12b. Distribution Code	
<b>DISTRIBUTION STATEMENT A</b> Approved for Public Release <b>Distribution Unlimited</b>			
<b>13. Abstracts :</b> The present final report concerns the original work undertaken at LABM to determine the boundary layer velocity distribution in the inboard region of a tiltrotor blade. The instrumentation consists in a Laser Doppler Velocimeter embedded in the inboard region of the blade. This unique set up allows measuring the chordwise and spanwise component of the boundary layer velocity from a distance of 0.3mm to 20mm along a direction normal to the blade surface. The experiments were carried out on a two bladed rotor with a blade geometry close to the one of CAMRAD II model of TRAM. The blade section located at $r/R=0.3$ was explored in three abscissa $x/C=0.10; 0.33; 0.54$ , and for 3 pitch angles, two of them at values lower than the static stall angle of incidence, the third at a higher value. During the tests the tip Mach number was maintained constant at $M_{tip}=0.22$ . Results obtained on the velocity components have allowed characterizing the different aspects of the BL. -At low incidences, chordwise velocity profiles exhibit a turbulent behavior (power law in $1/n$ ) for $x/C=0.33$ and $0.54$ . At the chord station $x/C=0.10$ , the BL is very thin with a laminar velocity profile. -At the incidence higher than the static stall one, it is worthy to note that the chordwise velocity profile at $x/C=0.3$ show an attached turbulent BL, while at $x/C=0.54$ the velocity profile begins to deviate from a turbulent shape to a separated one which produces the thickening of the BL and an evolution of the profile to a velocity distribution with an inflection point. This result confirms the delay of the BL separation due to rotation, already observed. At the leading edge ( $x/C=0.1$ ), and for the present low rotational speed $\Omega$ , the velocity distribution in the BL seems to point out a transitional zone ( $3 \leq \eta \leq 15$ ) inside of which the random of the velocity intensity attests of a high vorticity that may be due to a leading edge vortex or a bubble formation sustaining during the rotation the reattachment of the BL like observed at $x/C=0.33$ . The spanwise component is useful to precise if the flow passing over the blade section is centripetal or centrifugal, but the characterization of the BL behavior remains difficult to determine from the $V_r$ shape, except for transition and separation. The present results have shown that the ELDV is quite able to measure velocity profiles in the BL of a rotating blade and to qualify its nature. Complemented by results obtained in the future at higher tip Mach number, they will constitute a useful database for future computational unsteady boundary layer and CFD methods applied to tiltrotor blade aerodynamics.			
14. Subject terms: Tilt rotor blade			15. Number of Pages 18
			16. Price Code
17. Security Classification Unclassified	18. Security Classification of this Page Unclassified	19. Security Classification of Abstract Unclassified	20. Limitation of Abstract UL

## SUMMARY

Basic knowledge and numerical investigation of rotary wings aerodynamics request more and more accurate and suited experimental data. Particularly, phenomena occurring in the flow region very close to the blades, like transition, separation, and dynamic stall are highly dependent on the local boundary layer (BL). Improvement of recent computational works particularly concerned with tilt rotor blades needs to be strengthened by experimental data on local phenomena. In the inboard sections of a tiltrotor blade a stall delay is observed related to the delay of the boundary layer separation certainly due to rotational effect. Doubtlessly, experimental data on boundary layer velocity profiles are of evident interest for the phenomenological knowledge as well as for computational approach.

The present final report concerns the original work undertaken at LABM to determine the boundary layer velocity distribution in the inboard region of a tiltrotor blade. The instrumentation consists in a Laser Doppler Velocimeter embedded in the inboard region of the blade. This unique set up allows measuring the chordwise and spanwise component of the boundary layer velocity from a distance of 0.3mm to 20mm along a direction normal to the blade surface.

The experiments were carried out on a two bladed rotor with a blade geometry close to the one of CAMRAD II model of TRAM. The blade section located at  $r/R=0.3$  was explored in three abscissa  $x/C=0.10; 0.33; 0.54$ , and for 3 pitch angles, two of them at values lower than the static stall angle of incidence, the third at a higher value. During the tests the tip Mach number was maintained constant at  $M_{tip}=0.22$ .

Results obtained on the velocity components have allowed characterizing the different aspects of the BL.

-At low incidences, chordwise velocity profiles exhibit a turbulent behavior (power law in  $1/n$ ) for  $x/C=0.33$  and  $0.54$ . At the chord station  $x/C=0.10$ , the BL is very thin with a laminar velocity profile.

-At the incidence higher than the static stall one, it is worthy to note that the chordwise velocity profile at  $x/C=0.3$  shows an attached turbulent BL, while at  $x/C=0.54$  the velocity profile begins to deviate from a turbulent shape to a separated one which produces the thickening of the BL and an evolution of the profile to a velocity distribution with an inflexion point. This result confirms the delay of the BL separation due to rotation, already observed. At the leading edge ( $x/C=0.1$ ), and for the present low rotational speed  $\Omega$ , the velocity distribution in the BL seems to point out a transitional zone ( $3 \leq \eta \leq 15$ ) inside of which the random of the velocity intensity attests of a high vorticity that may be due to a leading edge vortex or a bubble formation sustaining during the rotation the reattachment of the BL like observed at  $x/C=0.33$ .

The spanwise component is useful to precise if the flow passing over the blade section is centripetal or centrifugal, but the characterization of the BL behavior remains difficult to determine from the  $V_r$  shape, except for transition and separation.

The present results have shown that the ELDV is quite able to measure velocity profiles in the BL of a rotating blade and to qualify its nature. Complemented by results obtained in the future at higher tip Mach number, they will constitute a useful database for future computational unsteady boundary layer and CFD methods applied to tiltrotor blade aerodynamics.

List of Keywords: Tiltrotor blade, Dynamic stall, Boundary layer separation, Embedded Laser Doppler Velocimeter.

## INTRODUCTION

Many aeronautics people have been fascinated during the past decades by the combination of vertical take off and landing with airplane flight offered by the tiltrotor aircraft configuration. Although Boeing has manufactured the V-22, an effort for improving the efficiency and the security of this new type of aircraft remains to be sustained. Analytical tools, as those developed by the Army/NASA rotorcraft Division at NASA-Ames, are devoted to calculate tiltrotor aeromechanical behavior (see ref.1). The validation of these calculations need more and more measured tiltrotor data, and comparison of measured and calculated aerodynamic characteristics have shown the lack of experimental informations on local phenomena as the stall delay observed in the inboard sections of tiltrotor blades. The delay of the boundary layer separation in these sections is certainly due to rotational effect<sup>2,3</sup>, and experimental data on boundary layer velocity profiles should be of evident interest.

LABM has developed for many years researches oriented towards the dynamic stall phenomenon simulated on oscillating airfoils (mainly in fore and aft motion at the beginning<sup>4</sup>, pitching and combined pitching and fore and aft later<sup>5</sup>), and towards the flow structure around helicopter rotor blades in hover and forward flight. These studies have allowed the improvement of original embedded LDV techniques for detailed and accurate measurements of the flow very close to moving walls and in their wakes<sup>6,7,8</sup>.

Concerning oscillating airfoils (NACA0012, 0.3m in chord), the velocity components have been measured<sup>8</sup> in 2D and 3D configurations by means of a LDV embedded in the oscillating frame, in such a way that the velocities are directly measured in a reference frame in relative motion.

Concerning hovering helicopter rotor blades<sup>6,7</sup>, BL measurements have been performed in a frame linked to the rotating blade for one radial distance from the rotation axis and at a chord abscissa  $x/c = 0.25$ . It has concerned the tangential velocity component (chordwise) and the crossflow component (spanwise). The boundary layer was explored at different rotating speeds of the blade. The accuracy of velocity components measurements has been evaluated in the region very close to the wall and far from the wall, showing that this new technique is well suited to unsteady measurement in the BL. Nevertheless, the instrumented blade was as geometrically simple as possible (untwisted) and of rectangular planform.

The purpose of the present research is to extend experiments based on the technique of the LDV embedded in the rotating geometrically simple blade to a more sophisticated blade with non linear twist and with chord thickness and profile spanwise distributions as close as possible to the blade tiltrotor characteristics. The geometry of the new blade is similar to the one of CAMRAD II model of TRAM<sup>1</sup>. The linear part of the twist in the inboard sections of the blade allows including an optical head and a 45 deg mirror located at the  $r/R$  station where converging laser beams emerge to focus at the measurement volume. The tangential and crossflow velocity components have then been measured in the boundary layer of the inboard section  $r/R=0.3$ , from 0.3mm to 20mm (corresponding to  $1 \leq \eta \leq 80$ ) along the normal direction, at several chordwise stations  $x/c=0.1; 0.33; 0.54$ .

The report presents successively the tilt rotor blade geometry adopted with the rotor hub used, and the experimental parameters. A detailed description of the LDV velocimeter and its embedment is given before showing how the velocity components (chordwise  $V_t$  and spanwise  $V_s$ ) are deduced from the measurements of the 2 components measured at +42deg and -37deg around the tangent to the blade section in the spanwise direction (as defined below).

The velocity results obtained at 3 pitch angles of the tested section (2 below the static stall angle  $\theta=10.22\text{deg}$  and  $15.38\text{deg}$ , the other above:  $\theta=24.75\text{deg}$ ) are then analyzed with respect to the

behavior of the boundary layer, in particular at high pitch angle where stall delay due to rotational effect should be observed.

### SYMBOLS

a	Speed of sound m/s
C	Airfoil chord, m
f	Rotational frequency, Hz
n	Rotational frequency in rpm
$M_{tip}$	Tip blade Mach number: $M_{tip} = \Omega R / a$
R	Rotor radius, m
Re	Reynolds number, $Re_f = \Omega r C / v$
$V_t$	Tangential velocity, m/sec
$V_r$	Crossflow velocity, m/sec, "+" centripetal, "-" centrifugal
$V_e$	External velocity at section $r/R=0.3$
s	Curvilinear abscissa, m
t	Time, sec
z	Normal distance to the surface of the blade section, mm
$\alpha$	Angle of attack of the blade section, deg
$\eta$	Reduced normal distance to the surface $= z(V_e/v_x)^{1/2}$
$\theta$	Pitch angle of the blade section
$\Omega$	Rotational frequency, rad/sec

### EXPERIMENTAL INVESTIGATION

#### The rotor blade geometry and the model scale of rotor

The geometry of the blade is similar to the one of CAMRAD II of TRAM<sup>1</sup>. In order to have the same solidity  $\sigma=0.1$  for a 2 bladed rotor, the following geometry of the blade has been adopted:

Rotor radius: $R=1.5\text{m}$
Blade length: $l=1.26\text{m}$
Solidity: $\sigma=0.1$
Number of blades: 2

Twist and chord distributions of the blade are respectively given in Table 1 and 2 and Fig 1 and 2. In Fig 1 the twist law distribution is presented with the conventional twist=0 at  $r/R=0.75$

TABLE 1

Spanwise section in % of R	Pitch angle in deg
15	0.000
20	-1.820
25	-3.610
30	-5.380
35	-7.140
40	-8.865
45	-10.500
50	-12.060
55	-13.550
60	-14.945
65	-16.280
70	-17.550
75	-18.750
80	-19.902
85	-20.990
90	-22.030
95	-23.020
100	-24.000

TABLE2

Spanwise section in % of R	Chord C/R
15	0.227
20	0.223
25	0.218
30	0.213
35	0.209
40	0.204
45	0.200
50	0.196
55	0.192
60	0.187
65	0.183
70	0.179
75	0.175
80	0.171
85	0.163
90	0.155
95	0.146
100	0.140

Twist

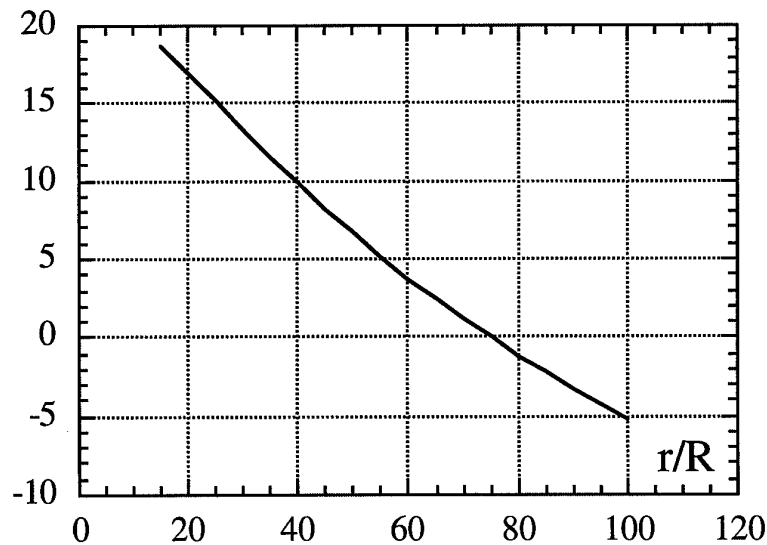


Fig.1 Twist distribution

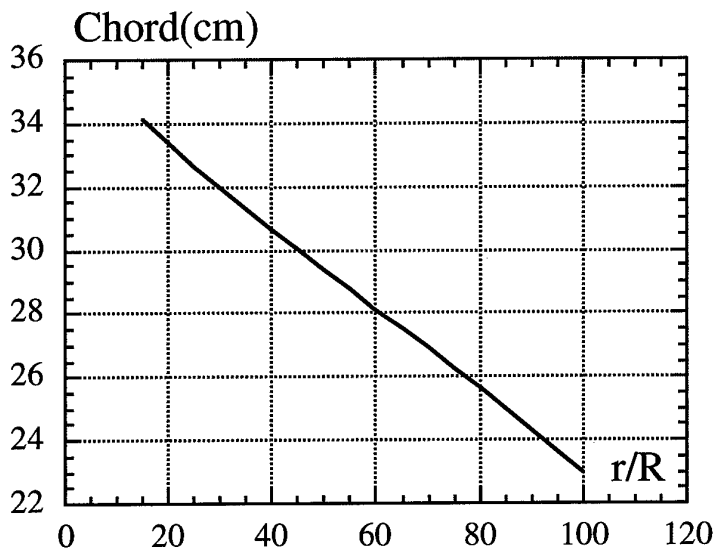


Fig.2 Chord distribution

Three different airfoils of NACA series have been distributed from the hub to the tip (NACA 64528, 64118, and 64152) as sketched at the top of Fig3.

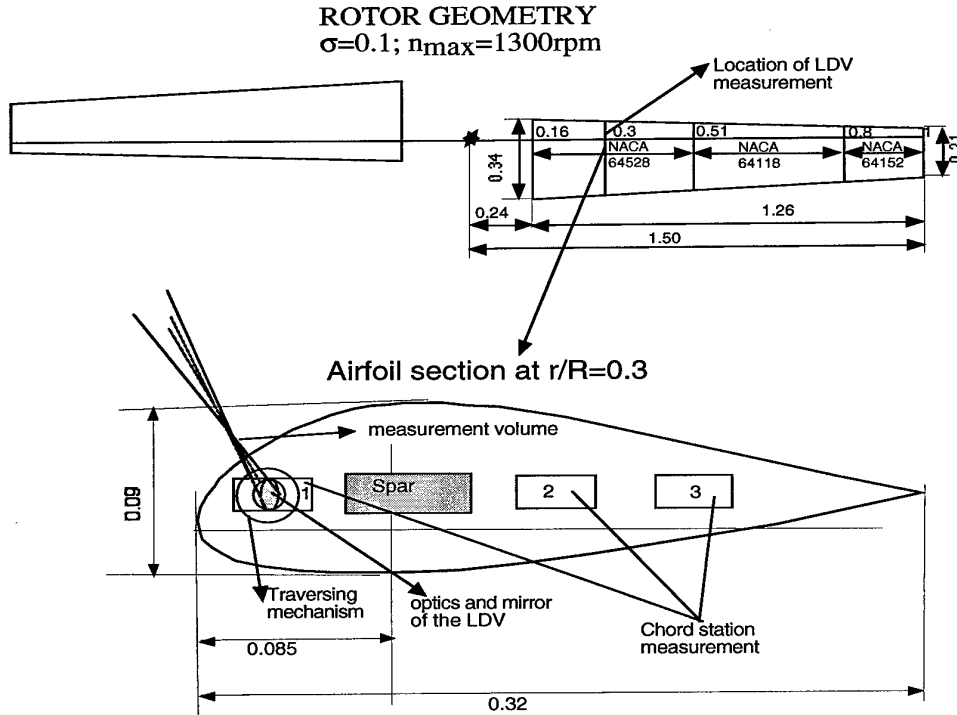


Fig 3. Rotor geometry and airfoil section characteristics.

The model scale of rotor is set up on the hovering test rig of LABM, located in the servicing hall ( $28 \times 16 \text{m}^2$ , 15m height) of the S1L wind-tunnel. The rotor hub is mounted vertically by means of a supporting mast with a center of rotation located at 2.9m above the ground. The model-rotor

consists of a fully articulated hub that can be equipped with interchangeable set of blades. The picture in Fig.4 shows the model rotor mounted in the hall of the S1L wind-tunnel. The rotor is operated in hover with an induced flow blowing from the bottom to the top in order to minimize the ground effect.

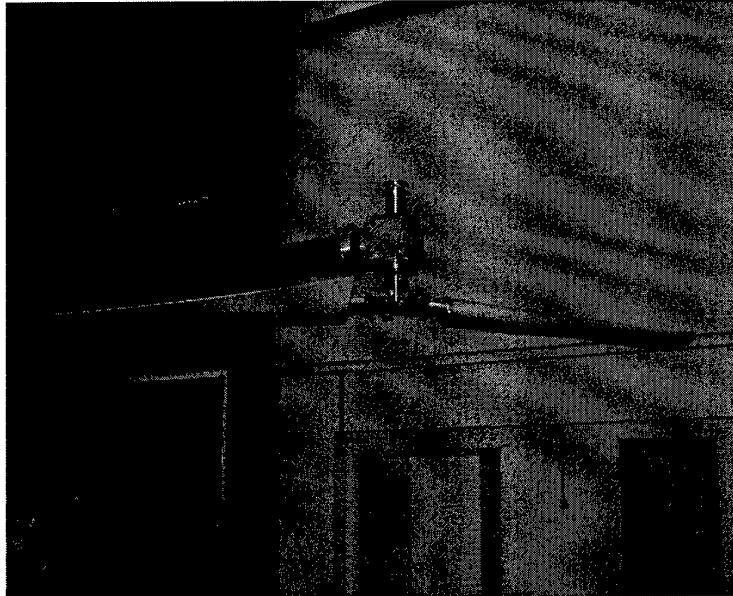


Fig 4. View of the rotor in the hall of S1L

#### Experimental apparatus: the Embedded LDV

The main components of the Laser Doppler Velocimeter are embedded in the rotating blade by use of a compact probe shown in Fig.5 and occupying about 0.22m in the span direction. The probe can be set in 3 different positions in chord noted 1,2,3 in the scheme of the bottom of Fig.3.

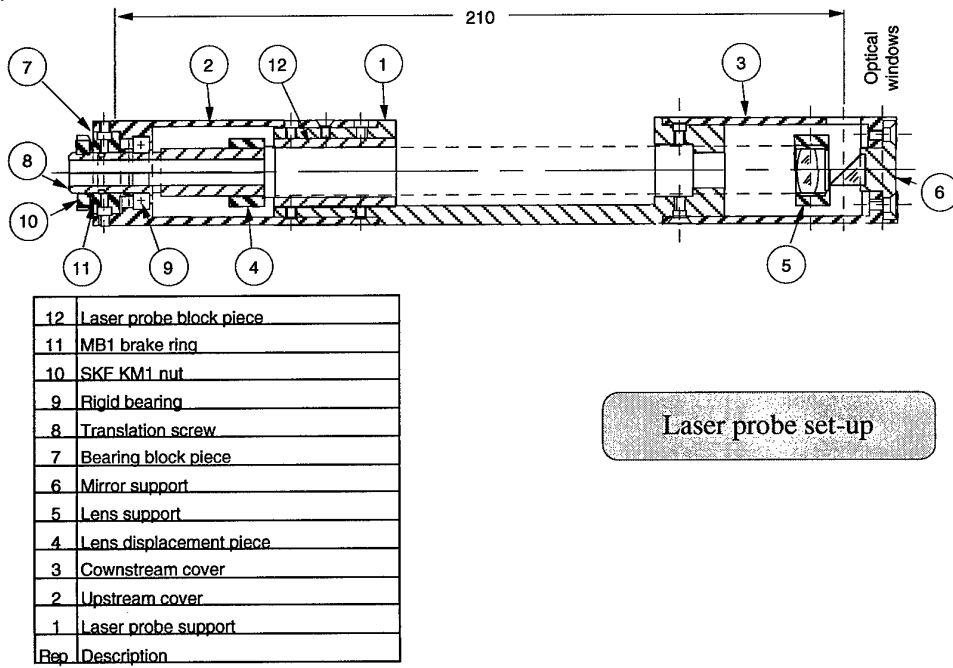


Fig.5 Embedded Laser probe set-up

Two parallel beams from the optical fibers arrive through the probe to the lens (5), converge to the mirror (6) and focalize through the optical window (mounted flush to the blade surface) in the measurement volume (see also Fig.3). This one can be displaced normally to the optical

window by means of the translation screw, which changes the relative position of the lens with the mirror. The more the lens is far from the mirror, the more the measurement volume is close to the blade surface.

The laser beams issued from the laser source are conducted to the blade through fixed optical fiber cables transmitting light by a transmitter to rotating optical fiber cables connected to the rotating blade by the guiding tube, the secondary gear box and the main gear box, as shown in the scheme of Fig.6. When particles seeding the flow pass through the measurement volume, the backscattered signals are collected through the rotating fiber optic cables to the fixed components of the velocimeter (photomultipliers, burst spectrum analyzer, computer, etc.).

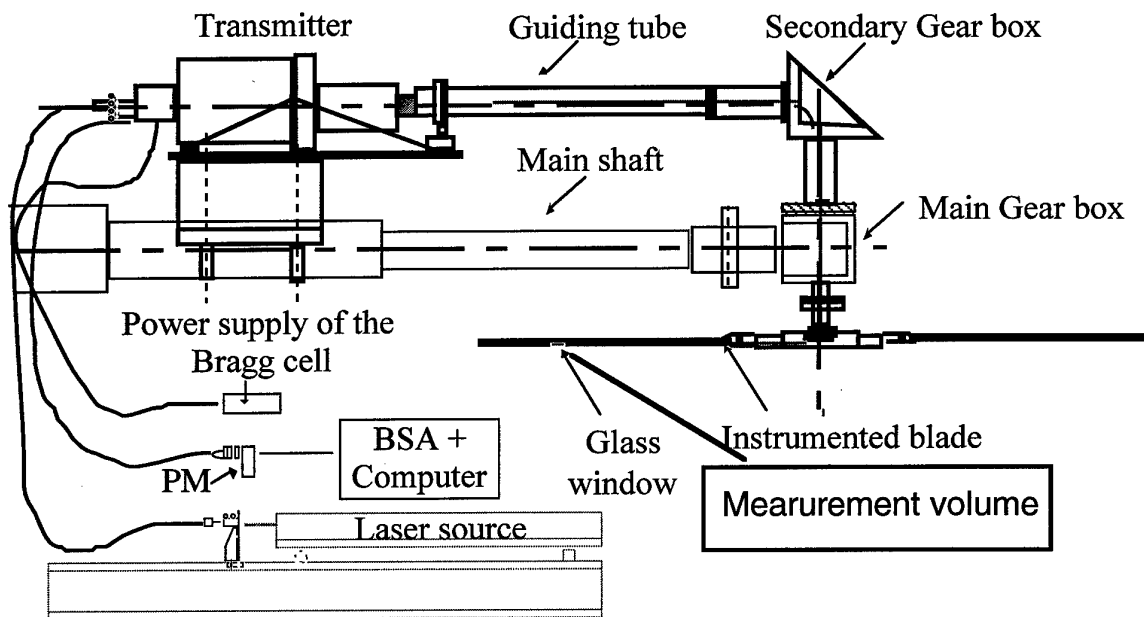


Fig.6. Schematics of the Embedded Laser Doppler Velocimetry method.

The picture in Fig.7 shows the laser beams focused in the measurement volume very close to the blade surface. The seeding of the flow is realized by oil smoke providing particles of about  $1\mu\text{m}$  in diameter.

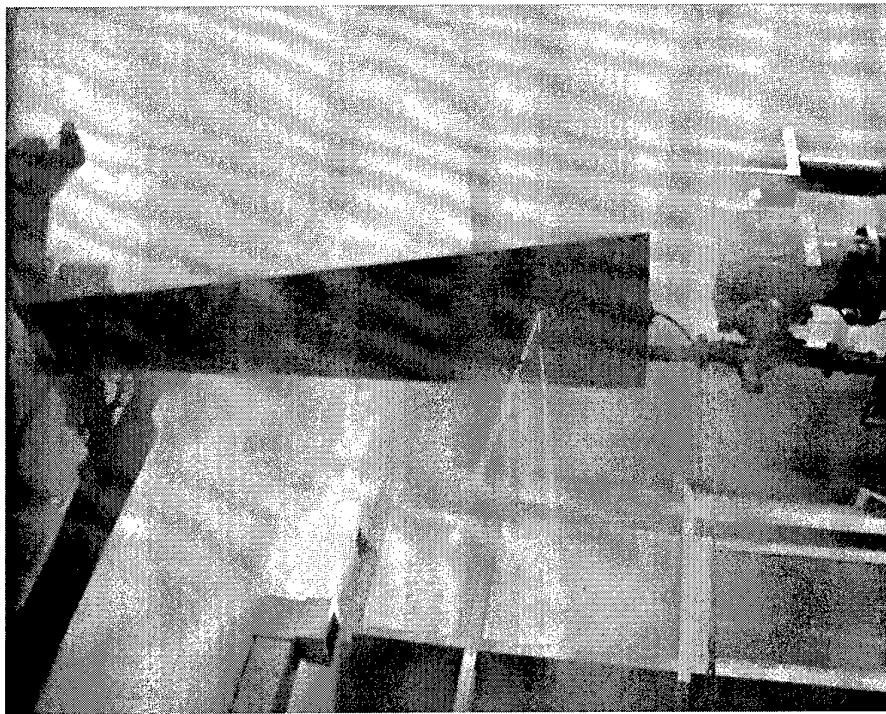


Fig 7. View of the blade and measurement volume

#### Measurement of velocity components $V_t$ and $V_r$

-The measurement volume: The following table gives the main characteristics of the velocimeter components with the dimensions of the measurement volume. The  $dz$  value allows a measurement at the wall as close as 0.3mm and the focal lens an exploration along the normal to the wall of 20 mm.

	Specification	Unit
Velocity component	1D*: tangential $V_t$ or spanwise $V_r$	m/s
Focal lens	50	mm
Laser source wave length	514,5	nm
Measurement volume	$dx=0.041$ $dz=0.510$	mm
Fringe spacing	0.0032	mm
number of fringes	13	
Axial working length	46	mm

-The seeding: A smoke generator is located on the floor of the hall under the rotor. The particles generated by a hot mixture of oil, manufactured by "Smoggy Fluid", have an average diameter of about  $1\mu\text{m}$

-The measured components  $U_{42}$  and  $U_{37}$  and the reconstruction of  $V_t$  and  $V_r$ : At each x/c the probe can be positioned in the same spanning hole in 2 different positions obtained by rotating the probe around its axis. By construction, in the first position the angle between the velocity component measured  $U_{42}$  and the chord direction is 42deg as the second position the angle with the chord direction is 37deg (see Fig.8).

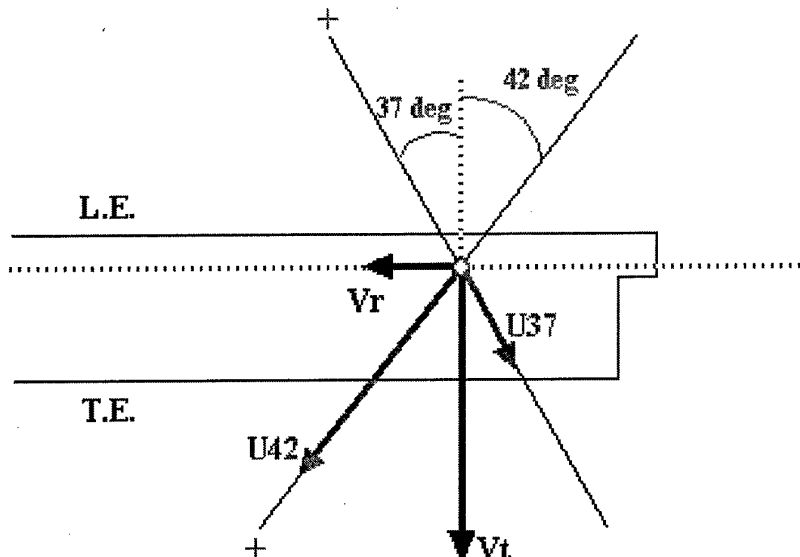


Fig 8. Principle of velocity measurements  $V_t$  and  $V_r$

With the adopted sign convention, the crossflow and chordwise components are given by the following equations:

Equations (1)

$$V_t = U_{42} \cos(42\text{deg}) - U_{37} \cos(37\text{deg})$$

$$V_r = -U_{42} \sin(42\text{deg}) - U_{37} \sin(37\text{deg})$$

-Data acquisition: Backscattered signals from the measurement volume are analyzed through BSA during a running time comprised between 3 seconds and 3 minutes, depending on the BL region explored. This time is used to acquire 4000 samples of the velocity components  $U_{42}$  or  $U_{37}$ . The data are recorded as presented in Fig.9 over a single period, and statistically treated (rms value, histogram, mean value,...). It can be seen that the seeding density is uniform along the period. The Fig 10 presents an example of histogram obtained with the  $U_{42}$  component.

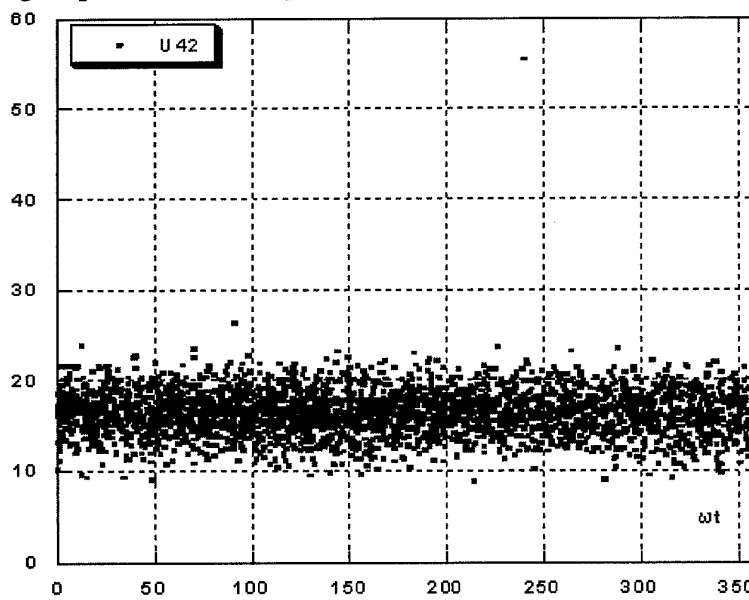


Fig 9. Example of  $U_{42}$  data acquisition presented over a single period (4000 data).  $\theta=10.2\text{deg}$  and  $x/c=0.54$

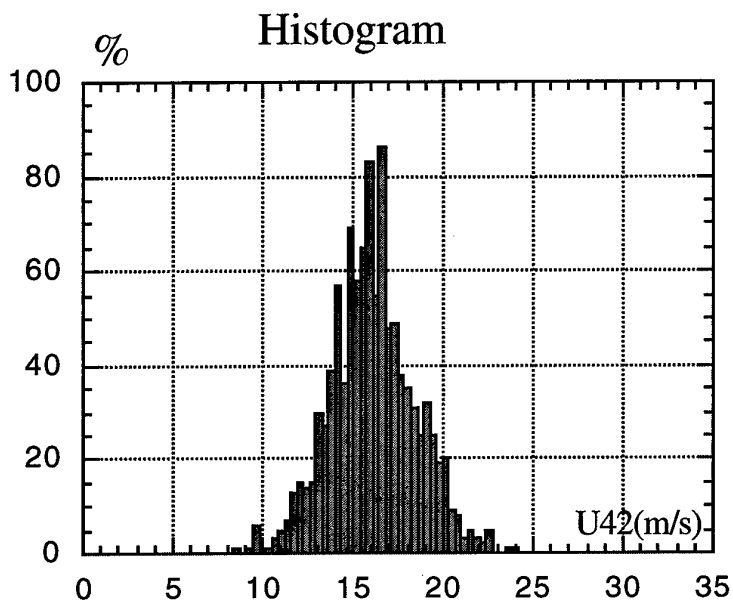


Fig.10. Example of histogram obtained with the  $U_{42}$  component.

The figure 11 presents an example of the variation with  $z$  of the  $U_{42}$  and  $U_{37}$  velocity components obtained as described above. Components  $V_t$  and  $V_r$  are then obtained from equations (1)

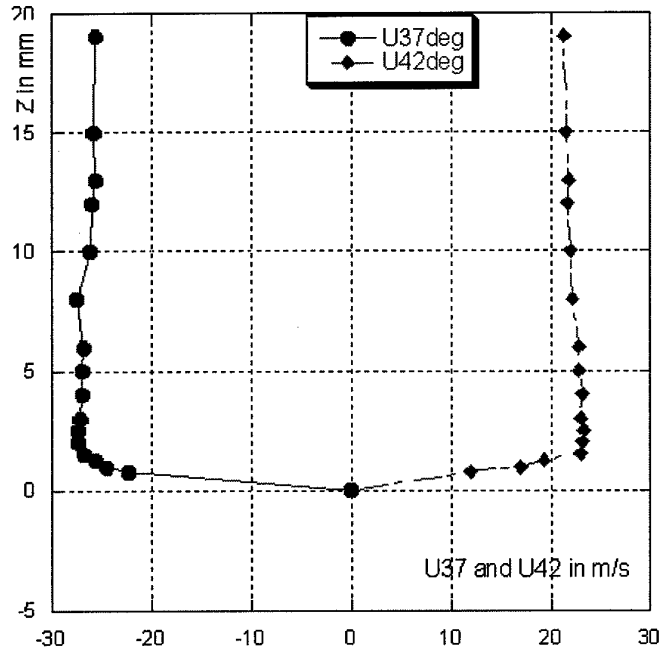


Fig 11. Evolution of the velocity component measured at  $\theta=15.38$  deg and  $x/c=0.33$

-Experimental uncertainty: the uncertainty of the ELDV used in a rotating blade has been evaluated in detail in Ref.9. It has been shown that the maximum measurement error on  $V_t$  is less than 2.6% and less than 6% concerning  $V_r$ .

## RESULTS AND DISCUSSION

### Test conditions

The first experiments were conducted at a relatively low speed rotation (480rpm). These “gentle” conditions have allowed to adjust with a high quality the embedded velocimeter method that required a long running time. Table 3 presents the test conditions and the corresponding data acquired:

<b>Table 3-Test conditions and data acquired : <math>r/R=0.3</math>; <math>n=580\text{rpm}</math>; <math>M_{\text{tip}}=0.22</math></b>			
Pitch angle $\theta_{r/R=0.3}$	10.22deg	15.38deg	24.75deg
Chord station $x/C$	0.1; 0.33; 0.54	0.1; 0.33; 0.54	0.1; 0.33; 0.54
Data acquired	$V_t$ ; $V_r$	$V_t$ ; $V_r$	$V_t$ ; $V_r$
Z explored in mm	0.3-19	0.3-19	0.3-19

The results analysis and particularly the aerodynamic behavior around the section airfoil enlightened by the BL velocity profiles require the knowledge of the angle of attack of the section airfoil obtained from the pitch angle and the induced incidence  $\alpha_i$  that can be deduced from the direct measurement of the induced velocity, or approximated from the Froude formula via the thrust coefficient  $C_T$ . Unfortunately, in the present study it was not preceded to forces nor induced velocity measurements through the rotor. Nevertheless, it is shown in Ref.1 that the TRAM calculated hover performance concerns values of  $C_T/\sigma$  varying from 0.06 to 0.14. Using the Froude formula, it can be deduced that:  $3\text{deg} \leq \alpha_i \leq 6\text{deg}$ . The angles of attack can be approximated to 7deg and 15deg, at low pitch angle  $\theta=10.22\text{deg}$ ; 15.38deg, and to 19deg at high pitch  $\theta=24.75\text{deg}$ .

Experimental results on  $V_t$  and  $V_r$  have been gathered in Fig.12 and 13. The couple ( $V_t$ ,  $V_r$ ) versus the distance to the wall  $z$  is displayed in Fig.12 for the three pitch angles  $\theta$ , and for the three chord stations  $x/C$  (respectively display A,B,C). Fig.13 presents the same data than Fig.12, where for each  $\theta$  (A,B,C), the display concerns  $x/C$ .

It can be seen from the analysis of Fig.12 that the chordwise component  $V_t$  increases with the incidence in the potential flow at each chord station (see A, B, C). This result, expected in the case of an unstall airfoil, becomes unexpected at  $\theta=24.75$ , where the angle of attack has been estimated at 19deg, incidence at which the BL should be separated. When examining the velocity profile in the BL at  $x/C=0.3$  (B), it can be said that the BL is attached and the shape of the profile is a turbulent one. At  $x/c=0.54$  (C), the profile in the BL has thickened with an evolution in  $z$  to an inflexion point, characteristic of a separation tendency. It seems that the BL has reattached at this high incidence by a leading edge process. Effectively, the acquisition of data relative to  $x/C=0.1$  have shown a particular behavior. The histogram relative to this high angle of attack conditions is given in Fig.14; the double pick seems to reveal a flow of particular vorticity or turbulence. The components  $U_{42}$  and  $U_{37}$  presented in Fig 15 exhibit a high degree of random in the potential flow, confirming the presence of a “transition” steady during the rotation due to a vortical zone or a bubble sustaining the flow attached at high incidence.

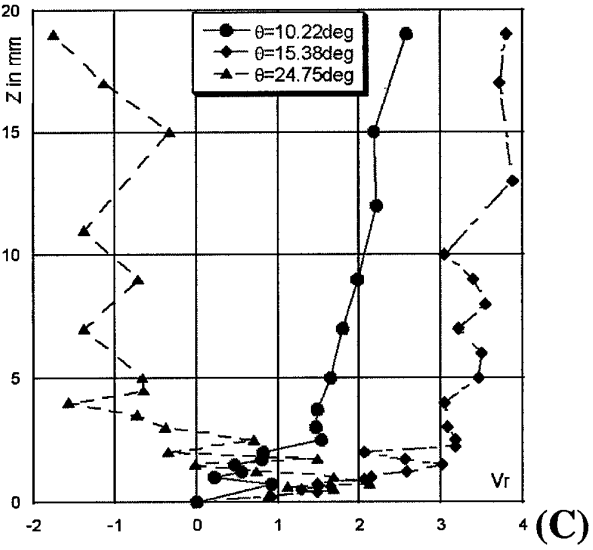
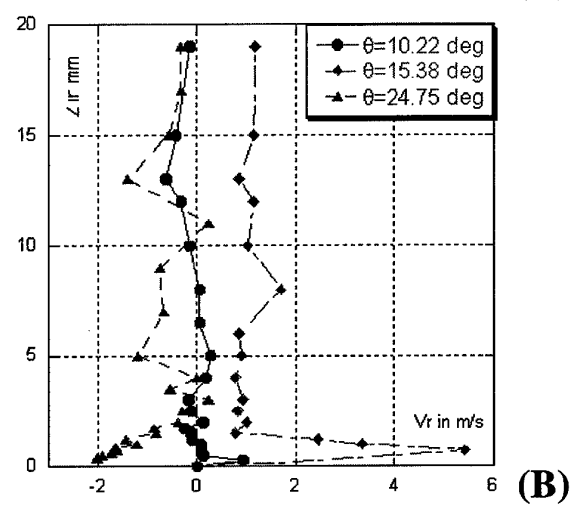
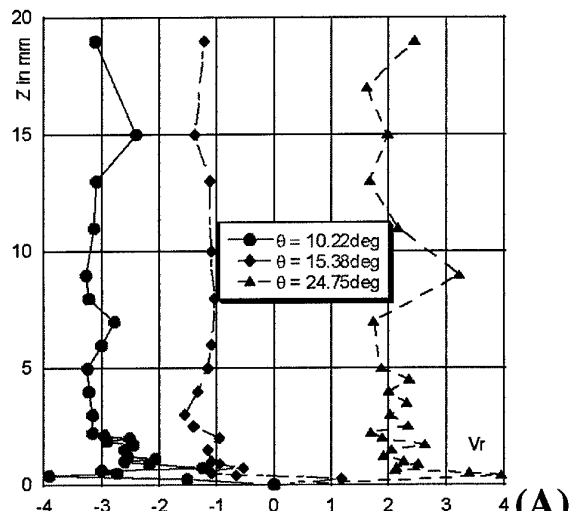
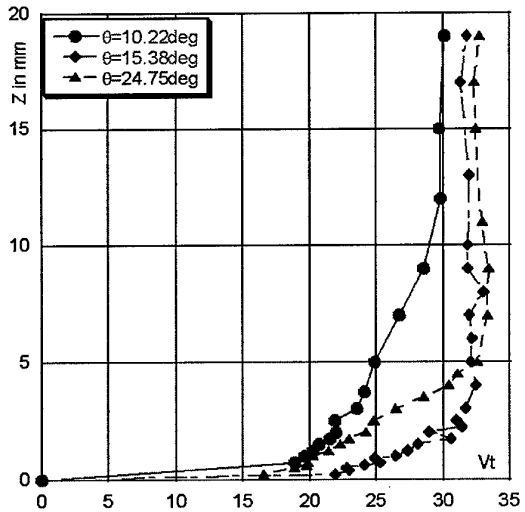
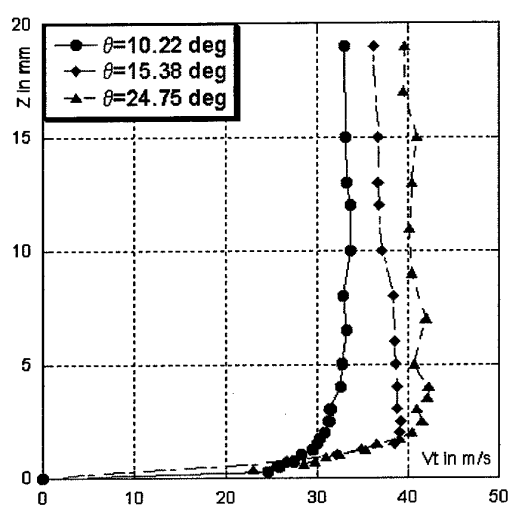
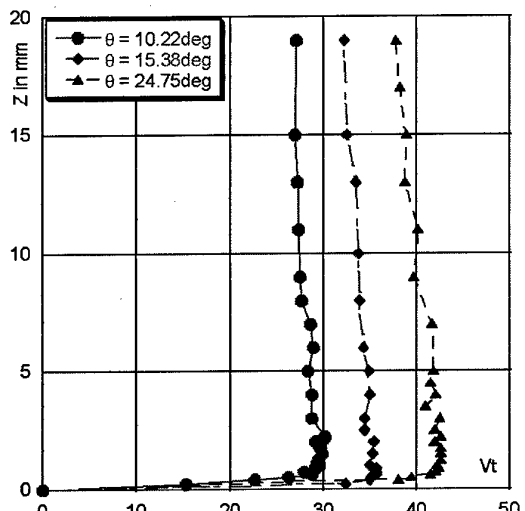


Fig.12 Evolution of  $V_t$  and  $V_r$  as a function of  $z$  for different  $\theta$  values at  $x/c=0.1, 0.33, 0.54$

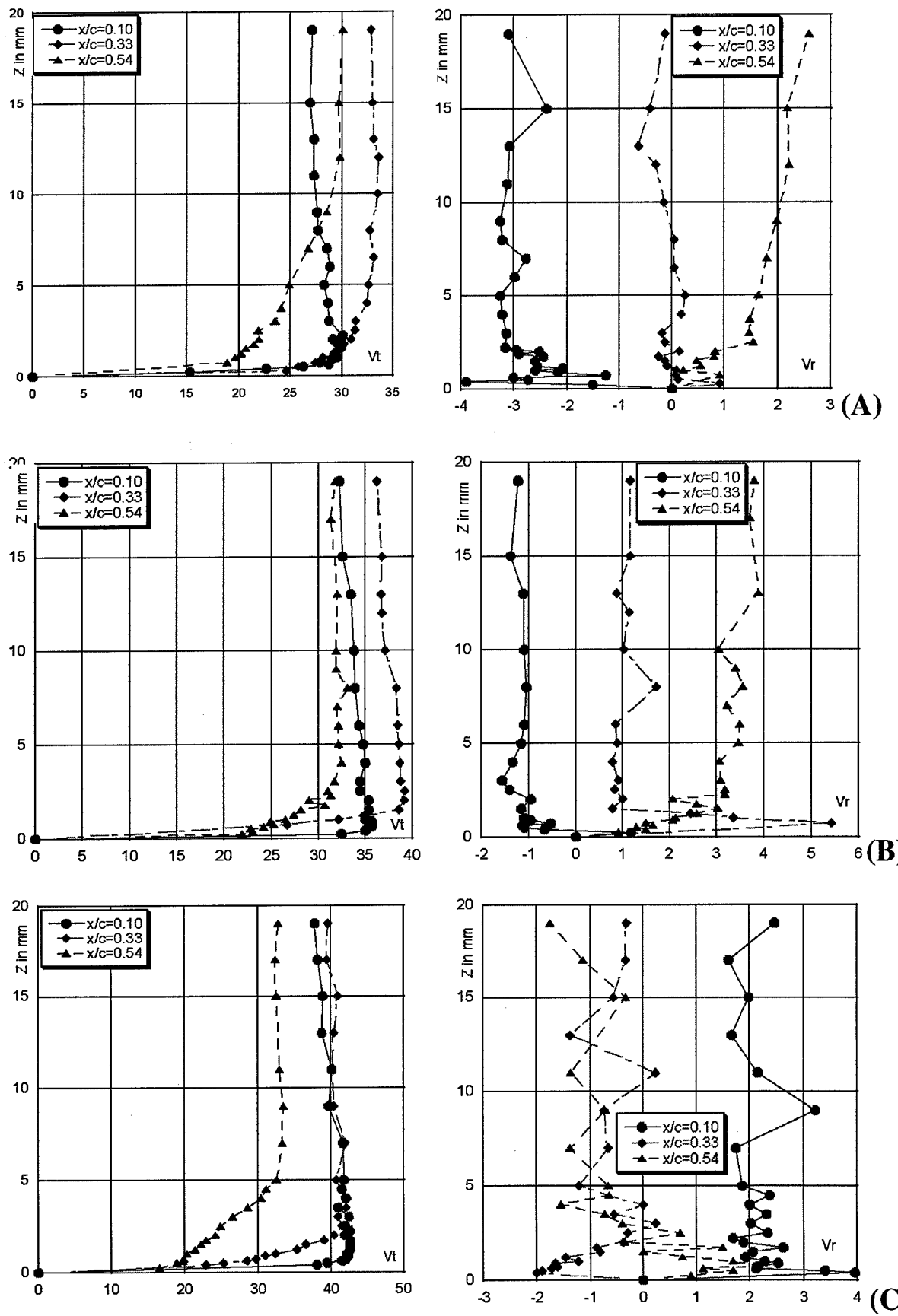


Fig.13 Evolution of  $V_t$  and  $V_r$  as a function of  $z$  for different  $x/c$  values at  $\theta = 10.22, 15.38, 24.75$  deg

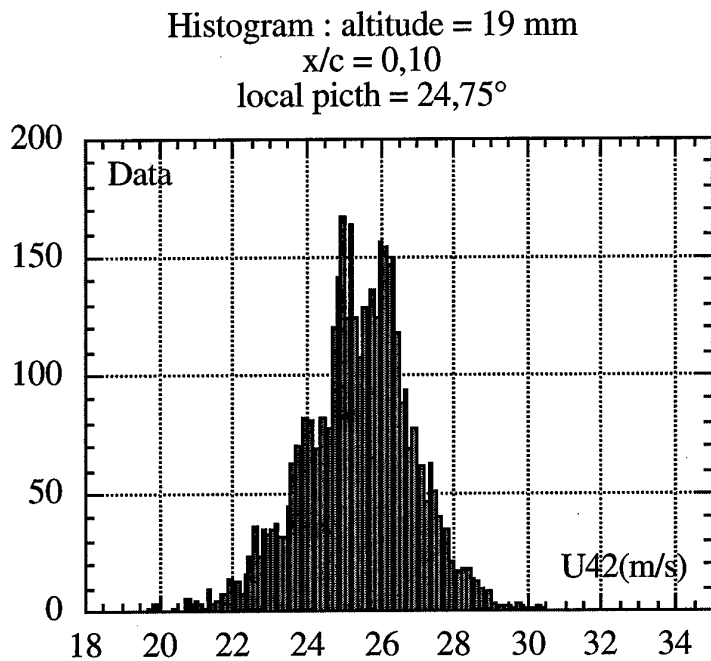


Fig.14 Example of histogram obtained on U42

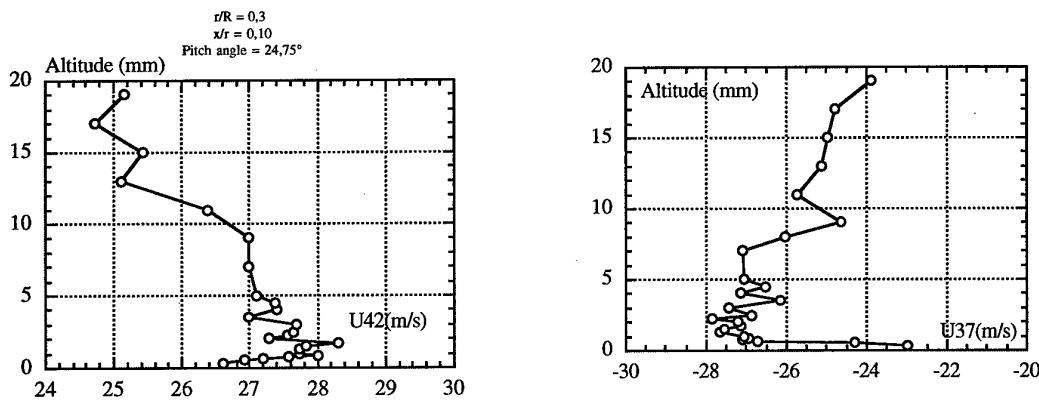


Fig.15 Evolution of the U42 and U37 components at  $\theta=24.75$

Concerning the behavior of the boundary layer at light incidence, the BL profiles  $V_t$  at the leading edge are characteristic of a laminar flow, while at  $x/c=0.33$  and  $0.54$ , they affect a turbulent shape. As an example, results obtained at  $\theta=10.33^\circ$  and  $x/C=0.54$ , presented in Fig. 16, are compared with success to a turbulent variation in  $1/n$  with  $n=5$ .

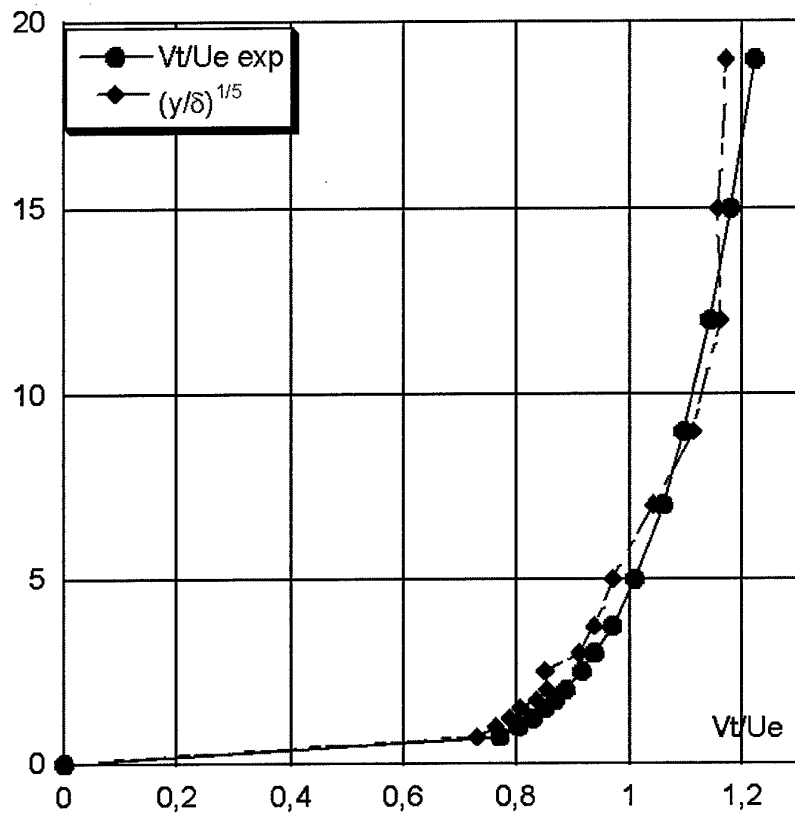
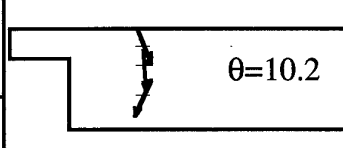
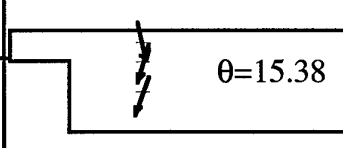
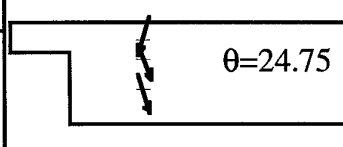


Fig.16 Comparison of  $(V_t/U_e)_{exp}$  with  $(y/d)^{1/5}$  for  $\theta=10.33\text{deg}$  at  $x/c=0.54$

The crossflow component remains difficult to analyze inside the BL because of the uncertainty of measurements on these quantities very close to the wall. Nevertheless, a better precision on  $V_r$  in the potential flow allows to obtain information on the direction of the flow at different station of the airfoil section. The following table 4 gives the centrifugal or centripetal tendency of the flow over the blade section, with on the right part the flow directions at different  $\theta$ , schematized by arrows.

Table 4 Evolution of the centrifugal forces as a function of  $\theta$  and  $x/C$

$x/C \backslash \theta$	10.22	15.38	24.75	
0.1	Centrifugal -3m/s	Centrifugal -1m/s	Centripetal 2m/s	
0.33	0	Centripetal 1m/s	Centrifugal -1m/s	
0.54	Centripetal 2m/s	Centripetal 3.5m/s	Centrifugal -1m/s	

## CONCLUSIONS

The boundary layer over the upper side blade surface of a tilt rotor has been explored by means of velocity measurements performed by an Embedded Laser Doppler Velocimeter (ELDV). The two bladed rotor has a geometry close to the one of CAMRAD II model of TRAM. Chordwise and spanwise components have been measured at the blade section  $r/R=0.3$ , for a constant tip Mach number  $M_{tip}=0.22$ , at three chord stations  $x/C=0.10; 0.33; 0.54$ , and for three pitch angles of the blade station  $\theta=10.22; 15.38; 24.75$ .

The analysis of the velocity components measured along the normal to the section airfoil in the BL and part of the potential flow, from 0.3mm to 20mm ( $1 \leq \eta \leq 80$ ), has pointed out the following conclusions:

- At low incidences, chordwise velocity profiles exhibit a turbulent behavior (power law in  $1/n$ ) for  $x/C=0.33$  and  $0.54$ . At the chord station  $x/C=0.10$ , the BL is very thin with a laminar velocity profile.
- At the incidence higher than the static stall one, it is worthy to note that the chordwise velocity profile at  $x/C=0.3$  shows an attached turbulent BL, while at  $x/C=0.54$  the velocity profile begins to deviate from a turbulent shape to a separated one which produces the thickening of the BL and an evolution of the profile to a velocity distribution with an inflection point. This result confirms the delay of the BL separation due to rotation, already observed. At the leading edge ( $x/C=0.1$ ), and for the present low rotational speed  $\Omega$ , the velocity distribution in the BL seems to point out a transitional zone ( $3 \leq \eta \leq 15$ ) inside of which the random of the velocity intensity attests of a high vorticity that may be due to a leading edge vortex or a bubble formation sustaining during the rotation the reattachment of the BL like observed at  $x/C=0.33$ .
- The spanwise component is useful to precise if the flow passing over the blade section is centripetal or centrifugal, but the characterization of the BL behavior remains difficult to determine from the  $V_r$  shape, except for transition and separation.

The present results have shown that the ELDV is quite able to measure velocity profiles in the BL of a rotating blade and to qualify its nature. Complemented by results obtained in the future at higher tip Mach number, they will constitute a useful database for future computational unsteady boundary layer and CFD methods applied to tiltrotor blade aerodynamics.

### Acknowledgment

The authors are particularly thankful to Dr. Chee Tung for his fruitful advices and encouragements during the work.

### References

- 1-Johnson, W., "Airloads and wake geometry calculations for an isolated tiltrotor model in a wind tunnel", Proc of 27<sup>th</sup> European Rotorcraft Forum, Moscow, Russia, September 11-14, 2001.
- 2-Corriigan, J.J., Schillings, J.J., "Empirical model for stall delay due to rotation". American helicopter society aeromechanics specialists conference, San Francisco, California, January 1994.
- 3-Du, Z., Selig, M.S., "A 3-D stall-delay model for horizontal axis wind turbine performance prediction". AIAA Paper 98-0021, January 1998.

4-Maresca, C., Favier, D., Rebont, J. "Experiments on an airfoil at high angle of incidence in longitudinal oscillations", Journal of Fluids Mechanics, Vol. 92, Part 4, pp. 671-690, 1979.

5-Favier, D., Maresca, C., Rebont, J. "Dynamic stall due to fluctuations of velocity and incidence" A.I.A.A. Journal, Vol.20, N°7, pp.865-971, 1982.

6-Favier, D., Maresca, C., Nsi Mba, M., Berton, E., Agnes, A., 1997, New Type of Embedded Laser Doppler Velocimeter (ELDV) for Measurement of Rotary Wings Boundary-Layer, The Review of Scientific Instruments, Vol. 66, n° 6, pp. 2447-2455.

7-Berton, E., Favier, D., Maresca, C., Nsi Mba, M., "Application of Laser Doppler Velocimetry to unsteady flow around rotating blades" Proc of 10<sup>th</sup> International Symposium on applications of laser techniques to fluid mechanics, Lisbon, 10-14 July 2000.

8-Maresca, C., Berton, E., Favier, D., Benyahia, A., "Study of 2D and 3D boundary layer of moving walls by embedded LDV measurements" Final Technical Report N° 68171-01-M-5090, ERO of the US Army, March 2002.

9-Deparis, M., « Application d'une technique de mesure basée sur la Vélocimétrie Laser Embarquée à l'étude de la couche limite développée sur une pale de rotor d'hélicoptère. » Thèse de Doctorat de l'Université d'Aix-Marseille II, 30 septembre 1998.